Supporting Information

In-situ self-assembly of molybdenum carbide and iron carbides heterostructure on N-doped carbon for efficient oxygen reduction reaction

Sagar Ingavale[1], Mohan Gopalakrishnan[1], Phiralang Marbaniang[2], Woranunt Lao-atiman[1], Ahmad Azmin Mohamad[3], Mai Thanh Nguyen[4], Tetsu Yonezawa[4], Anita Swami[5]*, Soorathep Kheawhom[1,6,7]*

[1] Department of Chemical Engineering, Faculty of Engineering, Chulalongkorn University, Bangkok 10330, Thailand

[2] Electrochemical Materials Lab, Faculty of Science (Chemistry), Ontario Tech University, Oshawa, ON L1G0C5, Canada

[3] Energy Materials Research Group (EMRG), School of Materials and Mineral Resources Engineering, Universiti Sains Malaysia, 14300, Nibong Tebal, Pulau Pinang, Malaysia

[4] Division of Materials Science and Engineering, Faculty of Engineering, Hokkaido University, Hokkaido 060-8628, Japan

[5] Department of Chemistry, SRM Institute of Science & Technology, Kattankulathur, Chennai 603203, India

[6] Center of Excellence on Advanced Materials for Energy Storage, Chulalongkorn University, Bangkok 10330, Thailand

[7] Bio-Circular-Green-economy Technology & Engineering Center (BCGeTEC), Faculty of Engineering, Chulalongkorn University, Bangkok 10330, Thailand

*Corresponding author Email: swamians@srmist.edu.in (Anita Swami), soorathep.k@chula.ac.th (Soorathep Kheawhom)

Characterization

The structural details of synthesized composites were evaluated using X-ray powder diffraction (XRD) measurements on X'pert pro diffractometer, PANalytical using CuK_α line (λ = 1.5406 Å 40 kV, 40 mA) in the 2θ range of 10^o – 80^o with scan rate 2^o/min. Raman spectroscopy (HORIBA, LABRAM HR Evolution) was studied using 633 nm laser excitation for the prepared composites. X-ray photoelectron spectroscopy (XPS) measurements were carried out using Shimadzu ESCA 3400 instrument with AlK_α source (Physical Electronics system; 1486.6 eV monochromatic beam) operated at 15 kV, and the XPSPEAK41 software was used for curve fitting and data analysis. A linear-type background was used for data processing. Further, a detailed SEM study was carried out using 'Quanta 200 FEG FE-SEM'. Transmission electron microscopy (TEM) images were taken on a JEOL Japan, JEM-2100 Plus microscope operated at 100 kV.

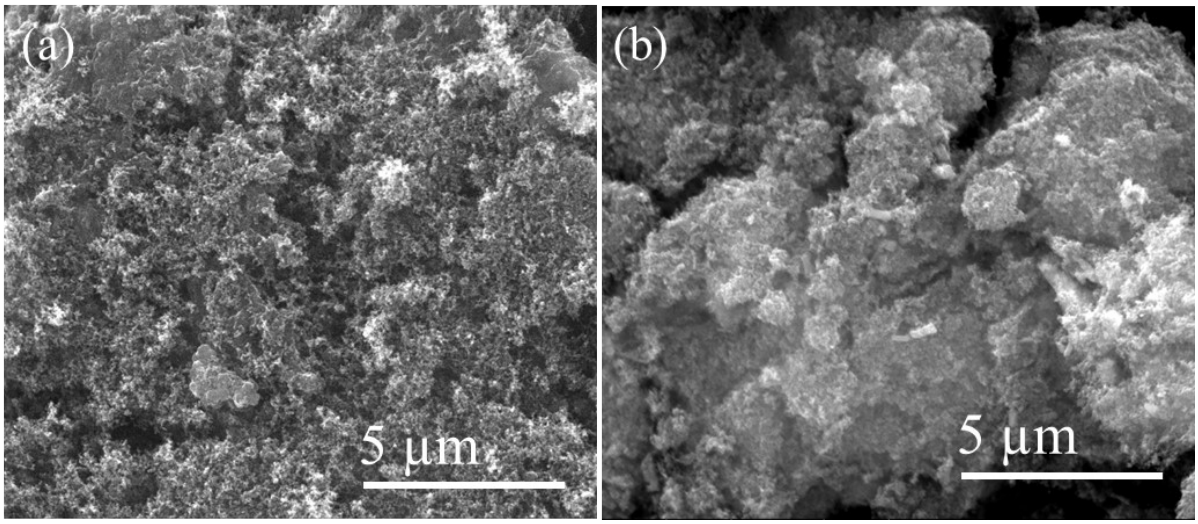

Figure S1. SEM images: (a) KBC, and (b) the Mo_2C/Fe_3C-NC3 catalyst.

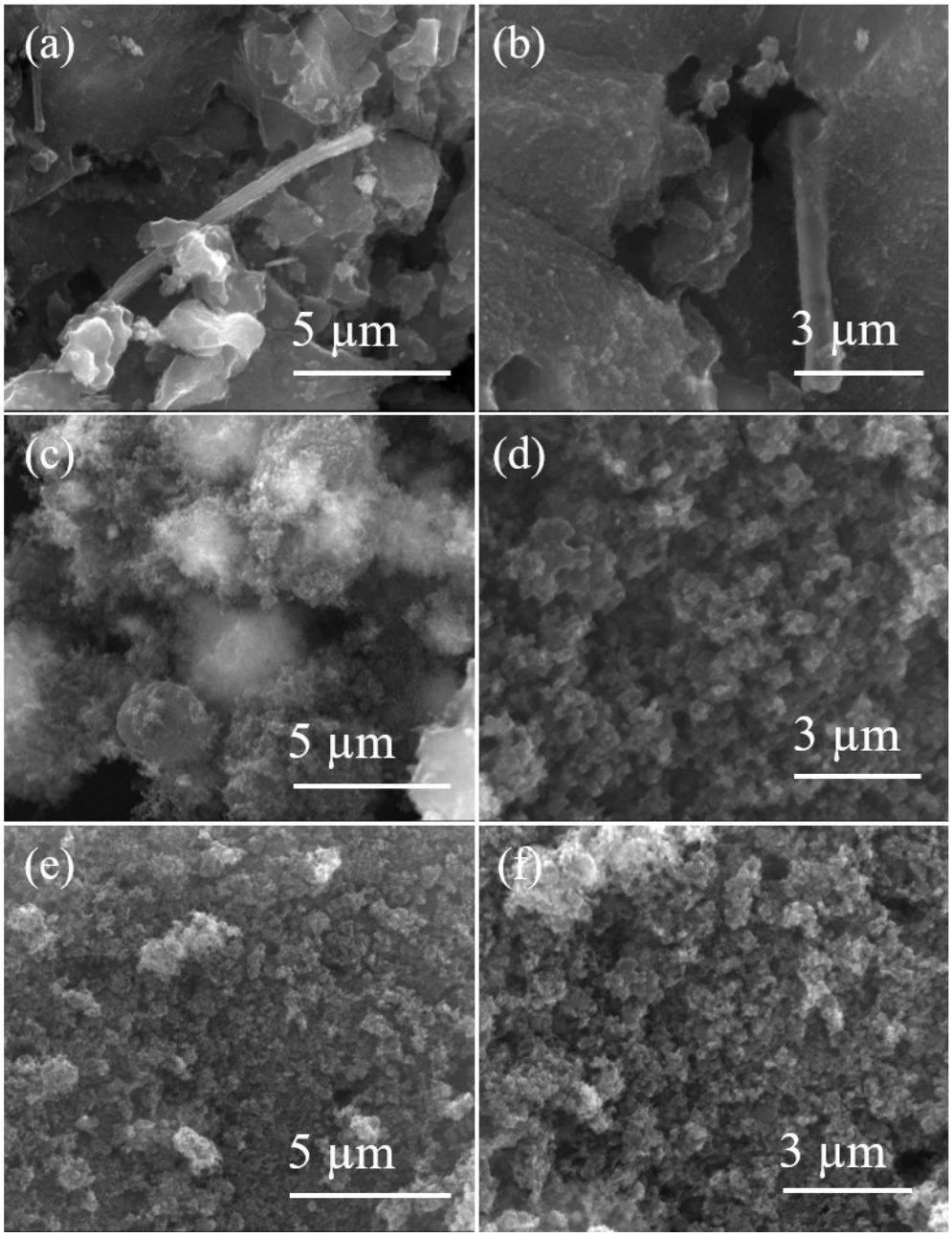

Figure S2. SEM images: (a, b) Mo_2C/Fe_3C catalyst, (c, d) MoO_2-C, and (e, f) Fe_2O_3-C composites.

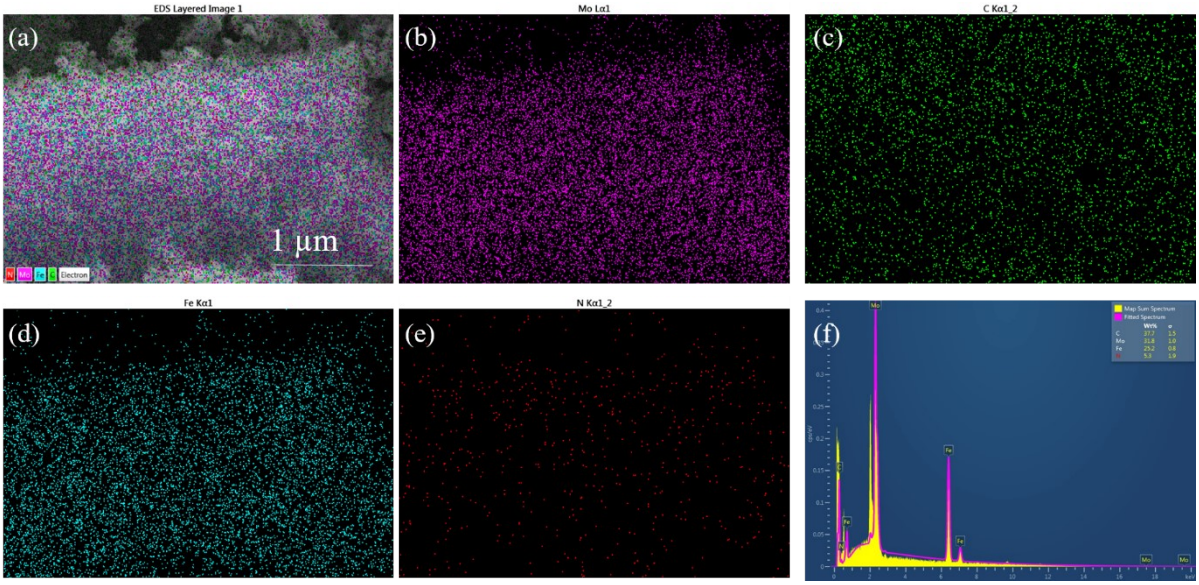

Figure S3. HR-SEM element mapping corresponds to (a) EDS layered image, (b) Mo, (c) C, (d) Fe, (e) N, and (f) EDS of Mo_2C/Fe_3C-NC3 composite.

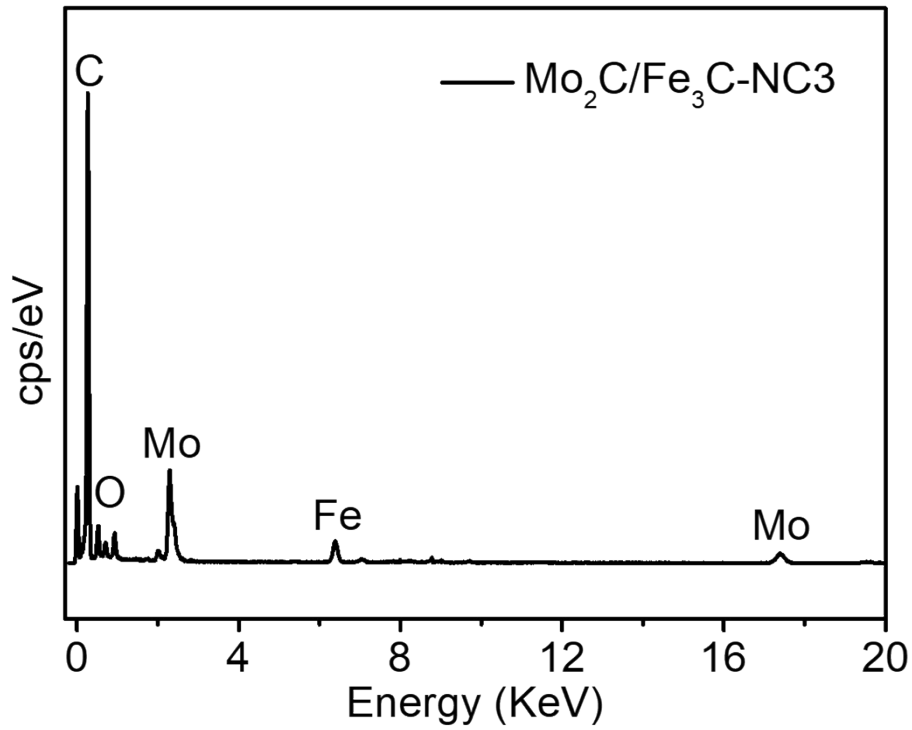

Figure S4. HR-TEM EDS spectrum of the prepared Mo_2C/Fe_3C-NC3 composite.

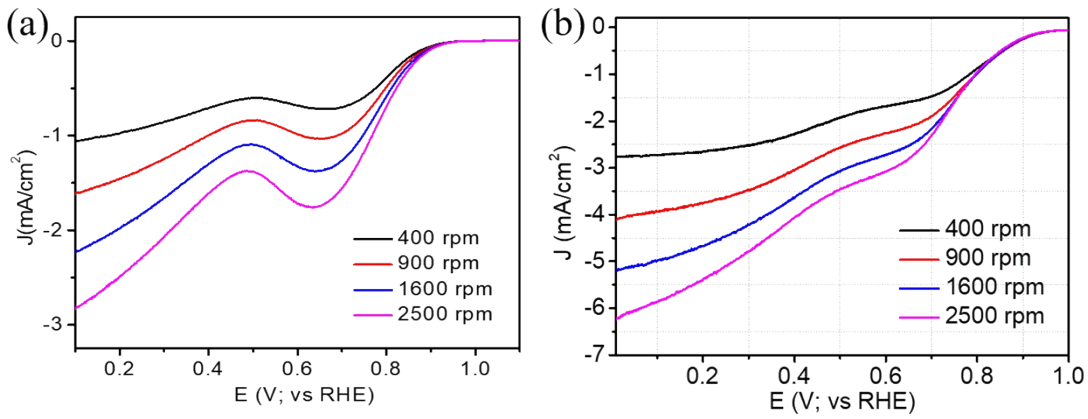

Figure S5. Polarization curves at different rotation: (a) KBC, and (b) Mo_2C/Fe_3C catalysts at scan rate 10 mV s^{-1}, in O_2 saturated 0.1 M KOH.

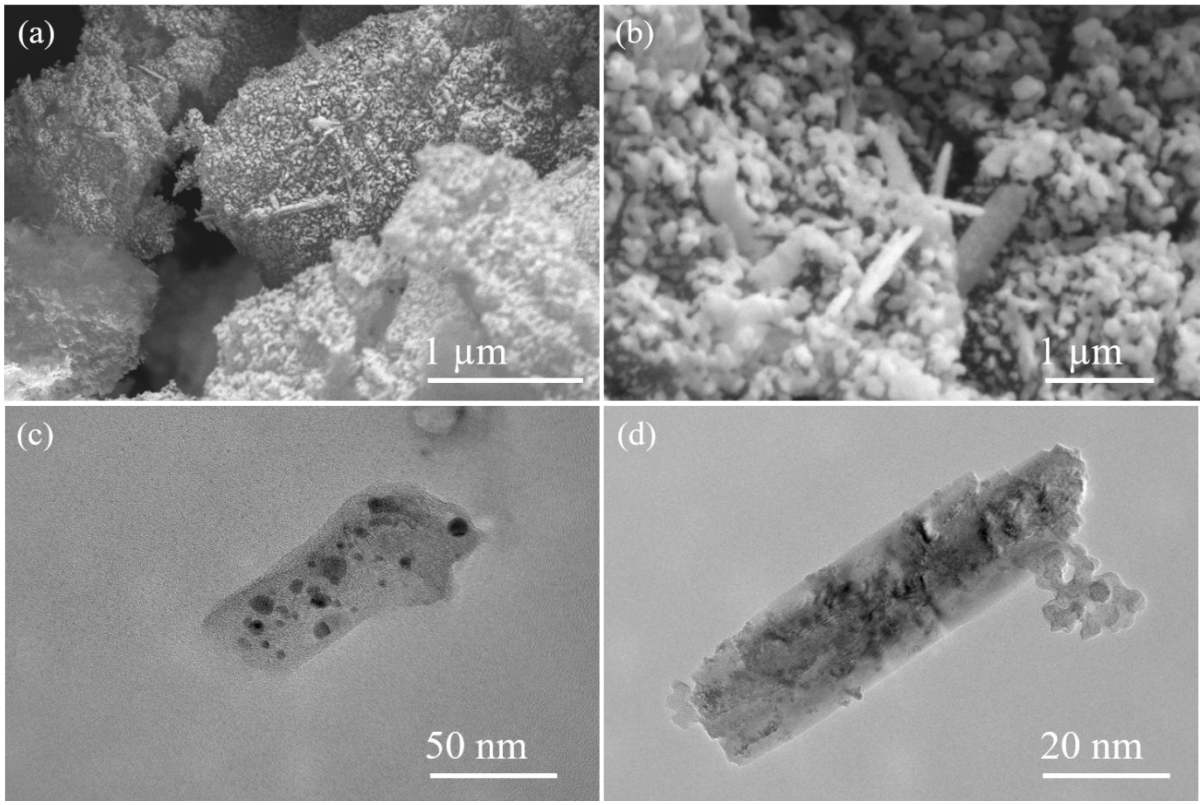

Figure S6. (a-b) SEM picture, and (c-d) low resolution TEM pictures for the Mo_2C/Fe_3C-NC3 composite after stability analysis.

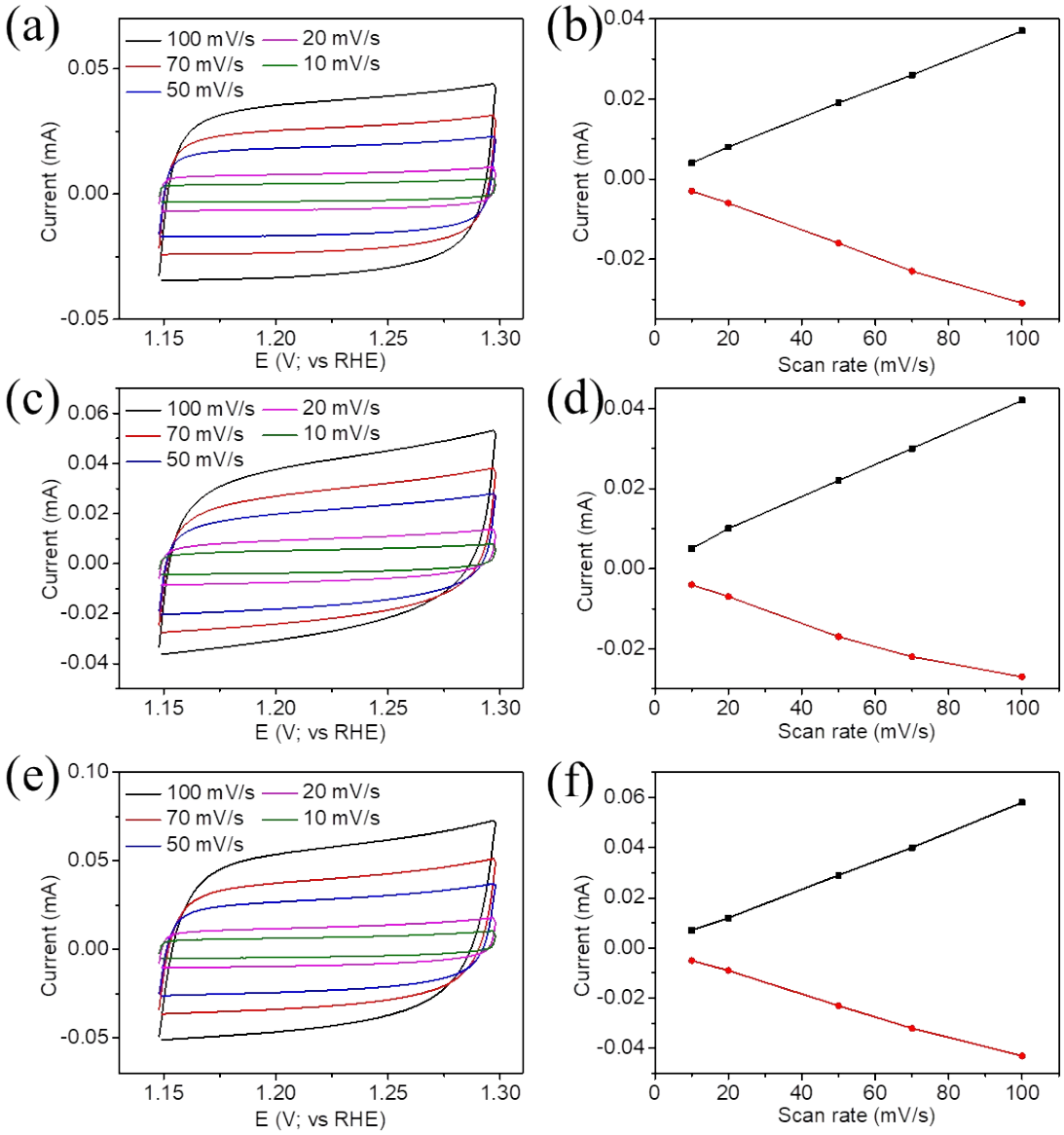

Figure S7. Comparative CVs and ECSA values: (a, b) MoO_2-C, (c, d) Fe_2O_3-C, and (e, f) Mo_2C/Fe_3C-NC3 catalysts.

Table S1. XPS analysis.

No.	Name of the element	Core binding energy (eV)	FWHM (eV)
1.	C 1s	283.7	0.9
		284.5	0.9
		285.1	1.6
		286.8	2.0
2.	O 1s	530.5	1.6
		532.0	2.3
		533.7	1.7
3.	Mo 3d	228.6	1.0
		231.9	1.3
		232.6	1.3
		235.7	1.3
4.	N 1s	398.4	1.6
		399.1	1.9
		400.7	2.1
5.	Fe 2p	707.5	1.8
		710.5	2.6
		721	2.9
		725.4	1.26

Table S2. Comparison of catalytic activity for the prepared catalysts.

No.	Catalyst	E_{onset} (V)	$E_{1/2}$ (V)	J_L (mA/cm^2)	Mass activity (mA/mg)
1.	MoO_2-C	0.89	0.76	4.2	38
2.	Fe_2O_3-C	0.95	0.8	5.6	83
3.	Mo_2C/Fe_3C-NC1	1.00	0.84	6.0	69
4.	Mo_2C/Fe_3C-NC2	0.97	0.86	5.9	139
5.	**Mo_2C/Fe_3C-NC3**	**1.00**	**0.89**	**6.2**	**221**
6.	Mo_2C/Fe_3C-NC4	1.00	0.88	5.5	190

Table S3. Comparison of ORR catalytic performances of Mo_2C/Fe_3C-NC3 with those of other reported electro-catalysts in alkaline media

No.	Catalyst	E_{onset} (V)	$E_{1/2}$ (V)	J_L (mA/cm^2)	Reference
1	Mo_2C/Fe_3C-NC3	1.00	0.89	6.2	This work
2	Mo_2C@NC/Co@NG-900	0.922	0.867	5.5	[1]
3	Mo_2C−GNR	0.93	0.8	4.6	[2]
4	Mo_2C/NCNT-30	0.85	0.62	4.22	[3]
5	MoC/NGr-3	0.93	0.80	3.091	[4]
6	Mo_2C/CXG	0.89	0.71	4.1	[5]
7	Mo_2C/NPCNFs	0.9	0.77	4.8	[6]
8	Fe-PANI@NP	0.85	0.72	4.5	[7]
9	Fe_3C/N,S-CNS	0.98	0.86	5.8	[8]
10	Fe-SAs/Fe_3C-Fe@NC	0.98	0.925	5.6	[9]
11	Fe_3C@N-CNTs	0.98	0.85	5.0	[10]
12	Fe_3C-Co-NC	1.02	0.89	4.5	[11]

References

1. Y. Wang, K. Li, F. Yan, C. Li, C. Zhu, X. Zhang and Y. Chen, *Nanoscale*, 2019, **11**, 12563-12572, 10.1039/C9NR02981H.
2. X. Fan, Y. Liu, Z. Peng, Z. Zhang, H. Zhou, X. Zhang, B. I. Yakobson, W. A. Goddard, III, X. Guo, R. H. Hauge and J. M. Tour, *ACS Nano*, 2017, **11**, 384-394, 10.1021/acsnano.6b06089.
3. Y.-J. Song, J.-T. Ren, G. Yuan, Y. Yao, X. Liu and Z.-Y. Yuan, *Journal of Energy Chemistry*, 2019, **38**, 68-77, 10.1016/j.jechem.2019.01.002.
4. H. Huang, C. Du, S. Wu and W. Song, *The Journal of Physical Chemistry C*, 2016, **120**, 15707-15713, 10.1021/acs.jpcc.5b10341.
5. D. Mladenović, M. Vujković, S. Mentus, D. M. F. Santos, R. P. Rocha, C. A. C. Sequeira, J. L. Figueiredo and B. Šljukić, *Nanomaterials*, 2020, **10**, 1805, 10.3390/nano10091805.

6. H. Wang, C. Sun, Y. Cao, J. Zhu, Y. Chen, J. Guo, J. Zhao, Y. Sun and G. Zou, *Carbon*, 2017, **114**, 628-634, 10.1016/j.carbon.2016.12.081.
7. R. Venegas, C. Zúñiga, J. H. Zagal, A. Toro-Labbé, J. F. Marco, N. Menéndez, K. Muñoz-Becerra and F. J. Recio, *ChemElectroChem*, 2022, **9**, e202200115, 10.1002/celc.202200115.
8. Q.-D. Ruan, R. Feng, J.-J. Feng, Y.-J. Gao, L. Zhang and A.-J. Wang, *Small*, 2023, **19**, 2300136, 10.1002/smll.202300136.
9. X. Sun, P. Wei, S. Gu, J. Zhang, Z. Jiang, J. Wan, Z. Chen, L. Huang, Y. Xu, C. Fang, Q. Li, J. Han and Y. Huang, *Small*, 2020, **16**, 1906057, 10.1002/smll.201906057.
10. L. Cui, Q. Zhang and X. He, *J. Electroanal. Chem.*, 2020, **871**, 114316, 10.1016/j.jelechem.2020.114316.
11. H. Wang, C. Sun, E. Zhu, C. Shi, J. Yu and M. Xu, *J. Alloys Compd.*, 2023, **948**, 169728, 10.1016/j.jallcom.2023.169728.